Anal. Chem. **2008,** *80,* 6974–6980

Contribution of Aquaporins to Cellular Water Transport Observed by a Microfluidic Cell Volume Sensor

Jinseok Heo,[†] Fanjie Meng,[‡] and Susan Z. Hua*[,†,‡]

Department of Mechanical & Aerospace Engineering, SUNY—Buffalo, Buffalo, New York 14260, and Department of Physiology and Biophysics, SUNY—Buffalo, Buffalo, New York 14214

Here we demonstrate that an impedance-based microfluidic cell volume sensor can be used to study the roles of aquaporin (AQP) in cellular water permeability and screen AQP-specific drugs. Human embryonic kidney (HEK-293) cells were transiently transfected with AQP3- or AQP4-encoding genes to express AQPs in plasma membranes. The swelling of cells in response to hypotonic stimulation was traced in real time using the sensor. Two time constants were obtained by fitting the swelling curves with a two-exponential function, a fast time constant associated with osmotic water permeability of AQP-expressing cells and a slow phase time constant associated mainly with water diffusion through lipid bilayers in the nontransfected cells. The AQP-expressing cells showed at least 10× faster osmotic water transport than control cells. Using the volume sensor, we examined the effects of Hg^{2+} and Ni^{2+} on the water transport via AQPs. Hg^{2+} inhibited the water flux in AQP3-expressing cells irreversibly, while Ni^{2+} blocked the AQP3 channels reversibly. Neither of the two ions blocked the AQP4 channels. The microfluidic volume sensor can sense changes in cell volume in real time, which enables perfusion of various reagents sequentially. It provides a convenient tool for studying the effect of reagents on the function and regulation mechanism of AQPs.

Water movement across the plasma membrane of cells is one of the fundamental processes in cell physiology, playing an important role in maintaining homeostasis of cell volume. While the lipid membrane is permeable to water, water transport is largely enhanced by the presence of water channels, called aquaporins (AQPs). AQPs are membrane protein channels that can selectively transport water molecules across the cellular membrane.[1] Up to date, 13 types of AQPs were identified from various animal tissues, plants,[2] and even bacteria.[3] It is reported that AQPs are closely associated with cell migration,[4] fat metabolism,[5] and neural signal transduction.[6] Malfunctioning of AQP can cause clinical diseases or disorder found in kidney,[7,8] respiratory tract,[9] brains,[10] and eyes.[11] The effect of AQP on water transport has been observed by using cells stably or transiently transfected with AQP-encoding genes[12] or AQP-knockout cells.[13] The regulation of AQPs' expression and their sensitivity to various substances have been the focus of recent studies. In order to better understand the role of AQPs in normal and pathological conditions and their regulation mechanisms, it is important to search for reagents that can selectively modulate AQP activities of different types in tissues or cells. So far, only a few pharmacological reagents have been known to interact with AQPs, and none of the known reagents is target-specific and toxic-free. Therefore, a convenient assay tool is required that can screen large commercially available libraries for AQP-specific drugs in high throughput.[14]

Since water molecules are neutral species, a traditional electrophysiology method, such as the patch clamp technique, cannot be employed to observe the water flux. Alternatively, the water permeability of AQP has been indirectly measured by tracing time-dependent volume change of the cells when subjected to an osmotic shock. Various techniques have been used to measure changes in the cell volume, including light scattering,[15] total internal reflection fluorescence,[16] confocal fluorescence micros-

* To whom correspondence should be addressed. Phone: (716) 645-2593, ext. 2358, Fax: (716) 645-3875. E-mail: zhua@eng.buffalo.edu.

† Department of Mechanical & Aerospace Engineering.

‡ Department of Physiology and Biophysics.

(1) Agre, P. *Angew. Chem., Int. Ed.* **2004**, *43*, 4278–4290.
(2) Kaldenhoff, R.; Fischer, M. *Acta Physiol.* **2006**, *187*, 169–176.
(3) Calamita, G.; Bishai, W. R.; Preston, G. M.; Guggino, W. B.; Agre, P. *J. Biol. Chem.* **1995**, *270*, 29063–29066.
(4) Saadoun, S.; Papadopoulos, M. C.; Hara-Chikuma, M.; Verkman, A. S. *Nature* **2005**, *434*, 786–792.
(5) Hara-Chikuma, M.; Sohara, E.; Rai, T.; Ikawa, M.; Okabe, M.; Sasaki, S.; Uchida, S.; Verkman, A. S. *J. Biol. Chem.* **2005**, *280*, 15493–15496.
(6) Nagelhus, E. A.; Mathiisen, T. M.; Ottersen, O. P. *Neuroscience* **2004**, *129*, 905–913.
(7) Chen, Y.-C.; Cadnapaphornchai, M. A.; Schrier, R. W. *Biol. Cell* **2005**, *97*, 357–371.
(8) Nielsen, S.; Kwon, T.-H.; Christensen, B. M.; Promeneur, D.; Frokiaer, J.; Marples, D. *J. Am. Soc. Nephrol.* **1999**, *10*, 647–663.
(9) Song, Y.; Verkman, A. S. *J. Biol. Chem.* **2001**, *276*, 41288–41292.
(10) Amiry-Moghaddam, M.; Ottersen, O. P. *Nat. Rev. Neurosci.* **2003**, *4*, 991–1001.
(11) Verkman, A. S. *Exp. Eye Res.* **2003**, *76*, 137–143.
(12) Preston, G. M.; Carroll, T. P.; Guggino, W. B.; Agre, P. *Science* **1992**, *256*, 385–387.
(13) Ma, T.; Yang, B.; Gillespie, A.; Carlson, E. J.; Epstein, C. J.; Verkman, A. S. *J. Clin. Invest.* **1997**, *100*, 957–962.
(14) Castle, N. A. *Drug Discov. Today* **2005**, *10*, 485–493.
(15) Fischbarg, J.; Li, J.; Kuang, K.; Echevarria, M.; Iserovich, P. *Am. J. Physiol. Cell Physiol.* **1993**, *265*, C1412−C1423.
(16) Farinas, J.; Simanek, V.; Verkman, A. S. *Biophys. J.* **1995**, *68*, 1613–1620.

10.1021/ac8008498 CCC: $40.75
Published on Web 08/13/2008

copy,[17] laser scanning reflection microscopy,[18] and interference filter methods.[19,20] While these techniques are sensitive enough to detect changes in the volume of a single cell, they are not suitable for high-throughput screening. We previously developed an impedance-based cell volume sensor that can measure changes in cell volume in real time.[21] The sensor offers fast and convenient introduction of different reagents, consumes a minuscule amount of reagents (<500 μL/test), and is straightforward to use and cost-effective.

In this paper, we report that the cell volume sensor can be used to study the water permeability of AQPs and to screen AQP-specific drugs. Two representative water channel proteins, AQP3 or AQP4, were overexpressed in human embryonic kidney-293 (HEK-293) cells by using a transient gene transfection method. We show that the sensor can resolve differences in the swelling kinetics between AQP-expressing cells and control cells and, therefore, allows the determination of the contribution of AQPs to cellular water transport. Heavy metal ions, Hg^{2+} and Ni^{2+}, were tested to examine their selectivity in inhibition of different types of AQPs. These results demonstrate that the volume sensor can provide a convenient platform for investigating the effect of reagents on the functions of AQPs.

EXPERIMENTAL SECTION

Chemicals. NaCl, KCl, $MgCl_2$, $NiCl_2$, and mannitol were purchased from Sigma-Aldrich (St. Louis, MO). *N*-2-Hydroxyethylpiperazine-*N*′-2-ethanesulfonic acid (HEPES) and $CaCl_2$ were obtained from Fisher Chemical (Fairlawn, NJ). $HgCl_2$ was purchased from Aceto Chemical (Flushing, NY). Transfection reagent was purchased from Roche Applied Science (FuGene 6, Indiana polis, IN).

Solution Preparation. A stock hypotonic solution was prepared consisting of 75 mM NaCl, 5 mM KCl, 2 mM $MgCl_2$, and 1 mM $CaCl_2$ in 10 mM HEPES solution at pH 7.4. The isotonic solution (340 mOsm) was prepared by adding mannitol to the stock hypotonic solution (176 mOsm). Because the sensor chip measures the conductance of a sensing chamber, the conductivity of the solutions was titrated to equality with NaCl. Different osmolarities of hypotonic solutions were prepared by changing the mixing ratio of the stock isotonic and hypotonic solutions. The final osmolarities of the solutions were measured using an osmometer (Advanced Model 303, Advanced Instrument, Norwood, MA).

Cell Culture and Transfection. Microscope slides were cut to fit in the sensor and coated with 50 μg/mL fibronectin solution in 50 mM TRIS buffer prior to cell seeding. HEK-293 cells (ATCC) were grown on the glass slide in a 35-mm Petri dish using Dulbecco's modified Eagle's medium containing fetal bovine serum and penicillin−streptomycin for 2−3 days. When the cells were 40−50% confluent on the glass, they were transfected with AQP3-GFP (AQP3 tagged with GFP at the COOH terminus of AQP3), GFP-AQP4 (AQP4 tagged with GFP at the NH_2 terminus of AQP4), and GFP-encoding plasmid DNA using lipid-based transfection reagent (FuGene 6) following the manufacturer's protocol. As a control, the cells were mock-transfected by using only transfection reagent. The expression of AQPs in the HEK cells was confirmed by observing the green emission of GFP using a fluorescence microscope (Axiovert 200M, Zeiss) and recorded using a CCD camera (Axiocam MRm, Zeiss). The filter set 38 HE (ex 470 ± 40 nm; dichroic filter 495 nm; em 525 ± 50 nm, Zeiss) was selected.

Measurement of Cell Volume Change. The microfluidic volume sensor was used to measure the cell volume change in real time.[21] The principle of measuring cell volume in our sensor is based on the fact that cells are electrical insulators at low frequencies. With cells in a chamber of fixed cross section, a change of cell volume displaces the extracellular fluid, thereby changing the chamber resistance. The sensing chamber is 17 μm deep and 1.5 mm wide connected to a fluid inlet and outlet. A glass slide containing the tissue cells was inverted over the sensor chip. The chamber resistance was measured using a four-electrode array providing sinusoidal current of 100 Hz, 200 nA. The voltage between the two inner electrodes was measured using an instrumentation amplifier with input currents of <1pA to reduce polarization. A lock-in amplifier provided rectification and filtering (A commercial version of this instrument, CVC-7000, is being manufactured by Reichert Instruments, Buffalo, NY). The sensing chamber was perfused with various solutions. The flow rate of the solution was controlled by adjusting hydraulic pressure at the inlet and measured at the outlet of the sensor. The data were plotted as the ratio of cell volume change to the resting cell volume as described in our previous report.[21]

RESULTS AND DISCUSSION

Measurement of Water Transport. Osmotic shocks were applied to HEK cells to cause water to transport across the cell membrane, and the subsequent changes in the cell volume were measured as a function of time using the volume sensor. Figure 1a shows a representative swelling curve of the HEK cells in response to a hypotonic stimulation (solid line). The chamber was initially perfused with isotonic solution (340 mOsm) and then switched to hypotonic solution (256 mOsm). The cells reached a maximum volume in the hypotonic solution in ~5 min, and the volume is ~30% larger than in the isotonic solution. For comparison, a solution exchange curve of the perfusing chamber was obtained by subsequently perfusing solutions with different conductivities in the chamber (Figure 1a (dashed line)). A complete characterization of solution exchange using various flow rates and the numerical simulation results have been published previously.[21] The time constants of the cell swelling and the solution exchange curves were obtained by fitting the data with an exponential function, and they were 60.3 and 3.2 s, respectively. These results show that the sensor can offer sufficient time resolution to observe the kinetics of cell swelling as a result of the osmotic water transport.

An initial response of cells to the hypotonic stimulus is the increase in cell volume due to the osmotic water transport. Extended hypotonic challenge may cause cells to release ions and osmolytes, resulting in a slow volume decrease, which is called

(17) Zelenina, M.; Brismar, H. *Eur. Biophys. J.* **2000**, *29*, 165–171.
(18) Maric, K.; Wiesner, B.; Lorenz, D.; Klussmann, E.; Betz, T.; Rosenthal, W. *Biophys. J.* **2001**, *80*, 1783–1790.
(19) Farinas, J.; Verkman, A. S. *Biophys. J.* **1996**, *71*, 3511–3522.
(20) Farinas, J.; Kneen, M.; Moore, M.; Verkman, A. S. *J. Gen. Physiol.* **1997**, *110*, 283–296.
(21) Ateya, D. A.; Sachs, F.; Gottlieb, P. A.; Besch, S.; Hua, S. Z. *Anal. Chem.* **2005**, *77*, 1290–1294.

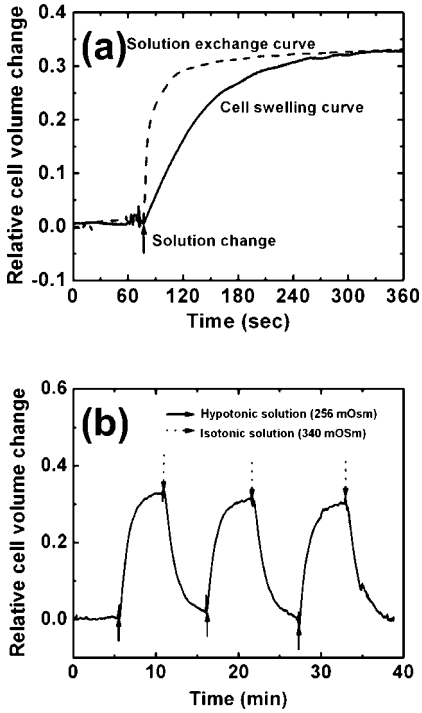

Figure 1. (a) Comparison of the rate of cell swelling in response to hypotonic challenge with the rate of solution exchange in the sensing chamber. The solution exchange curve was obtained by switching between two solutions having different conductivities. The curve was rescaled to compare with the cell swelling curve. (b) Volume change of HEK cells in response to the repeated challenges of hypotonic solution. The arrows indicate the solution switch.

regulatory volume decease (RVD).[22] This process normally takes 20−60 min in order to reach a steady-state cell volume.[21] Since the initial water permeability of cell membranes is the main concern of this work, a short duration of osmotic shocks was applied for the entire experiments. Figure 1b shows the change in cell volume in response to repeated hypotonic challenges of 5-min duration. We fitted each of those swelling curves with the exponential function and obtained reproducible time constants (τ_{av} = 60.6 ± 0.5 s, n = 3, the average value of the time constants obtained from the three swelling curves). This suggests that the water transport across the cell membrane is a reversible process during the cell swelling and shrinkage. In addition, the decrease in the magnitude of the maximum cell swelling was not significant during the repeated hypotonic perfusion, indicating that the cell did not lose electrolytes significantly.

Transfection of HEK Cells with AQP Genes. To clearly observe the contribution of AQPs to the water transport across cell membranes, either AQP3 or AQP4 was overexpressed in HEK cells. Panels a−c in Figure 2 show the fluorescence micrographs of HEK cells transfected with GFP, GFP-AQP3, and AQP4-GFP encoding genes, respectively. Figure 2d is the corresponding optical micrograph of Figure 2c. The HEK cells expressing only GFP showed homogeneous fluorescence intensity, which indicates that the GFP was mainly expressed in the cytosol (Figure 2a). On the contrary, AQP-expressing cells exhibited brighter fluorescence at the edges of the cell membranes (Figure 2b and c). The localized expression of AQPs in the plasma membranes can be more clearly observed using the confocal fluorescence microscope (see the Supporting Information). This suggests that the AQP3 and AQP4 channels were dominantly expressed in the plasma membranes, not in the cytosol. The expression of AQPs in the plasma membranes enables their participation in the water transport. Other cell lines, such as Chinese hamster ovary cells (CHO)[23] and lung epithelial cells,[24] also dominantly express the water channels in the plasma membranes.

Interestingly, small sizes of bright spots are more frequently observed in the AQP4-expressing cells than the AQP3-expressing cells (Figure 2b and c). This may be due to a unique property of AQP4 that can form clusters of orthogonal array of particles in the cell membranes.[25] The percentage of number of cells expressing AQPs among the total number of cultured cells can be estimated by comparing the fluorescence micrograph with its corresponding optical micrograph as shown in Figure 2c and d. Typically, 40−60% of the HEK cells displayed fluorescence after the transfection. The transfection efficiency for the HEK cells was much higher than for other cell lines, such as CHO and MDCK cells (<10%).

Contribution of AQPs on the Water Transport. We examined the effect of AQP- expression on the water transport in HEK cells using the cell volume sensor. Figure 3a shows typical swelling responses of AQP3- or AQP4-expressing cells in the hypotonic solution (256 mOsm) along with that of mock-transfected HEK cells. Note that the steady-state cell volumes are not very different from each other. The solution exchange curve in the empty chamber was also shown in Figure 3a for comparison (note that this curve was rescaled to compare with other cell swelling curves). Clearly, the initial swelling rate of AQP3- or AQP4-expressing cells was much faster than that of a mock-transfected cell. The time constant of water movement was commonly expressed using an exponential function regardless of the specific testing methods.[16,18] In order to observe the contribution of AQPs in the water transport across the cell membrane, an exponential function was used to fit the data measured using a volume sensor. Panels b and c in Figure 3 show the best fitting of swelling curves of AQP-expressing cells using a two-exponential function (eq 1).

$$R = R_0 - R_1 \exp(-t/\tau_f) - R_2 \exp(-t/\tau_s) \quad (1)$$

The time-resolved analysis of the swelling curve reveals that the water transport can be characterized using two time constants, i.e., fast time constant (τ_f) and slow time constant (τ_s). The mock-transfected cells was also fitted with the two-exponential function having the same time constants ($\tau_f = \tau_s$), as displayed in Figure 3d.

The τ_f value is associated with the swelling of AQP-expressing cells. Water transport through the AQPs is a dominant process for osmotic cellular water permeability in the AQP-expressing cells. Thus, the contribution of AQPs to the water movement was

(22) Lang, F.; Busch, G.; Ritter, M.; Volkl, H.; Waldegger, S.; Gulbins, E.; Haussinger, D. *Physiol. Rev.* **1998**, *78*, 247–306.
(23) van Hoek, A. N.; Yang, B.; Kirmiz, S.; Brown, D. *J. Membr. Biol.* **1998**, *165*, 243–254.
(24) Zelenina, M.; Bondar, A. A.; Zelenin, S.; Aperia, A. *J. Biol. Chem.* **2003**, *278*, 30037–30043.
(25) Yang, B.; Brown, D.; Verkman, A. S. *J. Biol. Chem.* **1996**, *271*, 4577–4580.

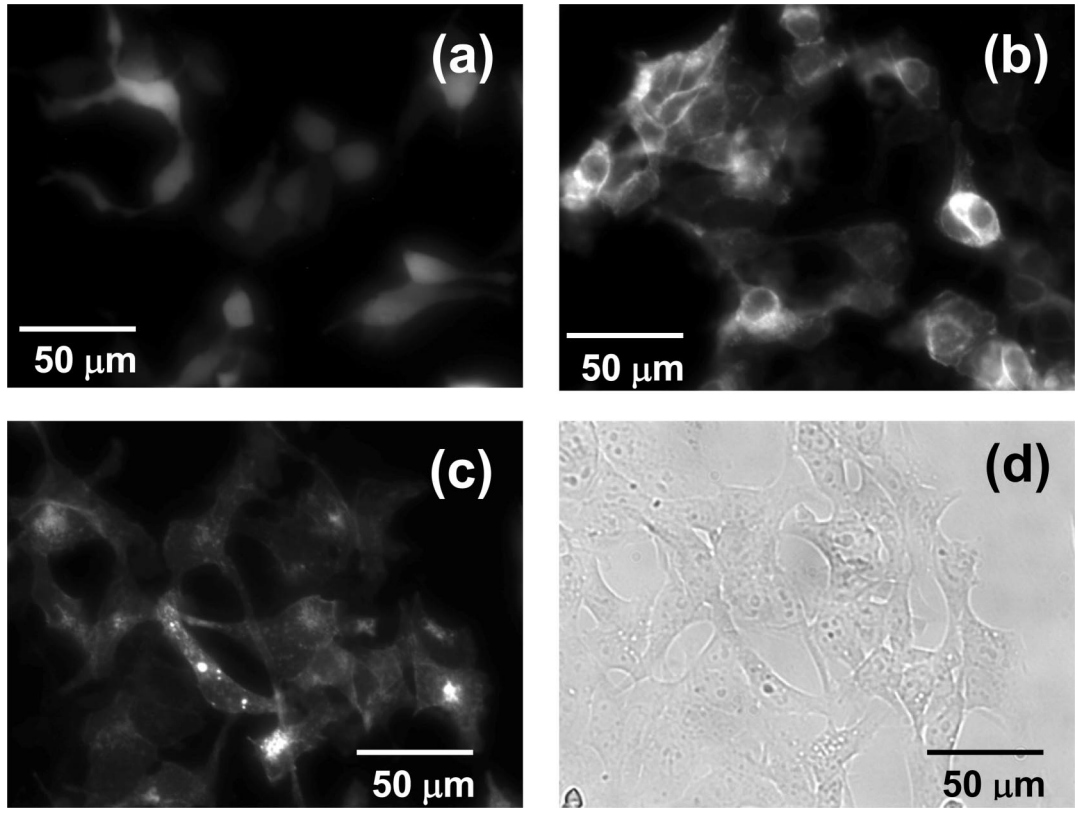

Figure 2. Fluorescence micrograph of HEK-293 cells: (a) transfected with GFP-encoding genes; (b) transfected with GFP-AQP3 encoding genes; (c) transfected with AQP4-GFP encoding genes. (d) Corresponding optical micrograph of AQP4-expressing HEK cells in Figure 2c. All images were obtained with 40× objective lens.

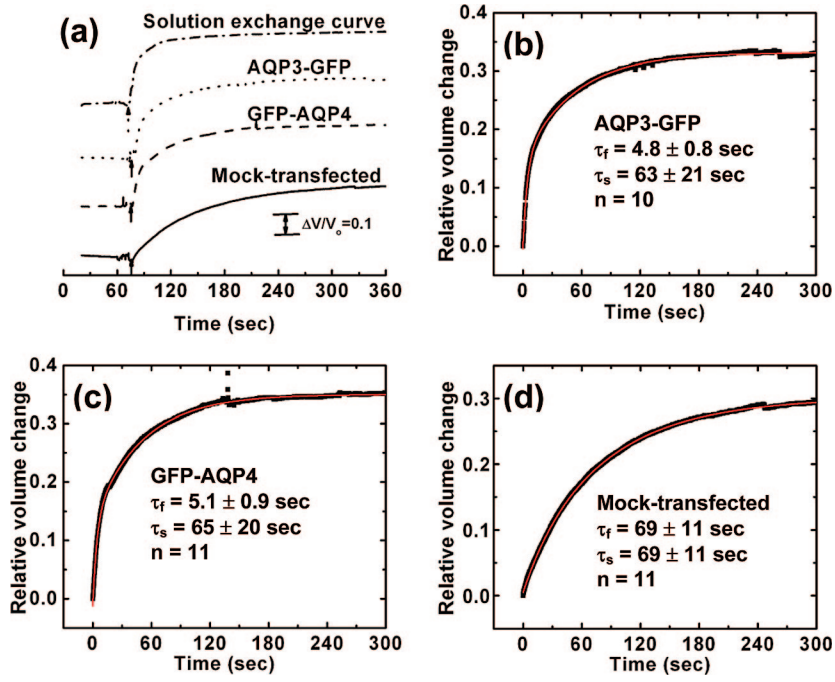

Figure 3. (a) Cell swelling curves of AQP3-, AQP4-expressing, and mock-transfected HEK cells along with the solution exchange curve in the empty chamber. The responses of cells were obtained by perfusing the chamber with a hypotonic solution of 256 mOsm. The solution exchange curve was obtained by switching between two solutions having different conductivities. The curve was rescaled to compare with the cell swelling curve. (b) Curve fitting to cell swelling of AQP3-expressing HEK cells. (c) Curve fitting to cell swelling of AQP4-expressing HEK cells. (d) Curve fitting to cell swelling of mock-transfected HEK cells. The τ_f and τ_s values were fast and slow time constants, respectively, obtained from fitting the curves with a two-exponential function (See the main text for details.). The values shown here are the average time constants measured from 10 or 11 independently prepared samples.

estimated by comparing the τ_f value for the AQP-expressing cells with that for the mock-tranfected cells. The average values of the fast time constants (τ_f) for the AQP3-expressing cells (n = 10 differently prepared samples) and the AQP4-expressing cells (n

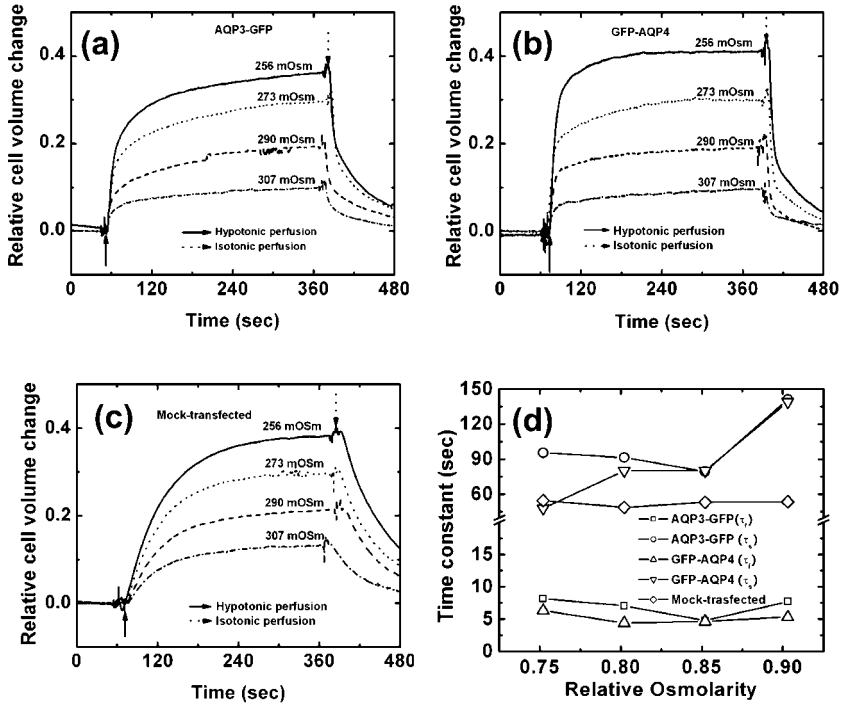

Figure 4. Dependence of swelling curves on the hypotonic osmolarity of AQP3-expressing HEK cells (a), AQP4-expressing HEK cells (b), and mock-transfected HEK cells (c). (d) Graph showing the effect of hypotonic osmolarity on the time constants.

= 11) were 4.8 ± 0.8 and 5.1 ± 0.9 s, respectively, while the average time constant for the mock-transfected cells was $\tau_f = 69 \pm 11$ s ($n = 11$). The water transport rate was enhanced more than 10-fold after the AQP-gene transfection, suggesting that the AQPs are dominant water pathways for the initial swelling in the AQP-expressing cells. Note that we cannot obtain the intrinsic water permeability of AQP-expressing cells since the fast time constants (~5 s) are comparable to the solution exchange time (~3 s). However, the substantial difference in the apparent time constants between the transfected and nontransfected cells makes it possible to observe the contribution of AQPs and the effect of drugs on the AQP's water permeability using the sensor. For future applications, the solution exchange time of the empty chamber can be improved to subsecond range by reducing the size of the sensing chamber, also by placing a drain channel more closely before the sensing chamber to allow complete removal of the dead volume prior to applying a new solution. Previously, another group has reported that the single-channel water permeability of AQP4 is ~3 times faster than that of AQP3.[26] However, because the collective water permeability depends on the number of AQP channels expressed in the cells, we cannot directly compare our data with the single-channel water permeability. The transfection reagent did not affect the water permeability of the cells, because the time constants of mock-transfected cells ($\tau_f = 69$ s) are comparable to those of wild-type HEK cells ($\tau_f = 60.6$ s). In the case of mock-transfected or wild type cells, the water permeability is associated with the transport through the endogenous AQPs and lipid membranes.

The slow water transport, characterized by τ_s, may reflect the swelling kinetics of nontransfected cells. The average values of the slow time constant (τ_s) for the AQP3- and AQP4-expressing cells and mock-transfected cells were 63 ± 21 ($n = 10$), 65 ± 20 ($n = 11$), and 69 ± 11 s ($n = 11$), respectively. The coincidence of the time constants suggests that the slow time constant component of the swelling is mainly associated with the water diffusion through lipid bilayers in nontransfected cells. Note that the late phase of cell swelling may also involve the movement of ions and other osmolytes across the cell membrane leading to RVD.[22]

The ratio of R_1 to $R_1 + R_2$ from eq 1 reflects transfection efficiency. The average values of the ratio for the AQP3- and AQP4-transfected cells were 0.45 ± 0.14 ($n = 10$) and 0.41 ± 0.15 ($n = 11$), respectively, which is in general agreement with the estimation from the fluorescence micrographs. Since variations in the transfection efficiency only affect the preexponential factors, not the apparent time constants, our analysis for the AQP's water permeability based on the time constants is valid regardless of the transfection efficiency.

We also examined the dependence of water permeability on the osmotic pressure gradient for the cells with and without AQP expression. Panels a−c in Figure 4 show the changes in cell volume in response to different hypotonic osmolarity. Each panel of Figure 4 was generated using the same cell culture with sequential hypotonic challenges of different osmolarities. Following each hypotonic challenge, isotonic solution was perfused to restore the cell volume to the resting volume before new hypotonic solution was introduced to the chamber. The initial rates of the swelling and shrinking events were almost identical as shown from Figures 4a to c. This indicates that only reversible water transport is involved in those early phases of cell swelling or shrinking. In contrast, the swelling and shrinking curves at the late phase look different. This discrepancy may be due to the hysteresis of cytoskeletal rearrangement or the difference in the activated ionic transport pathways between the swelling and shrinking events. Here we only considered the time constants of the swelling curve. The effect of different hypotonic osmolarity on the

(26) Yang, B.; Verkman, A. S. *J. Biol. Chem.* **1997**, *272*, 16140–16146.

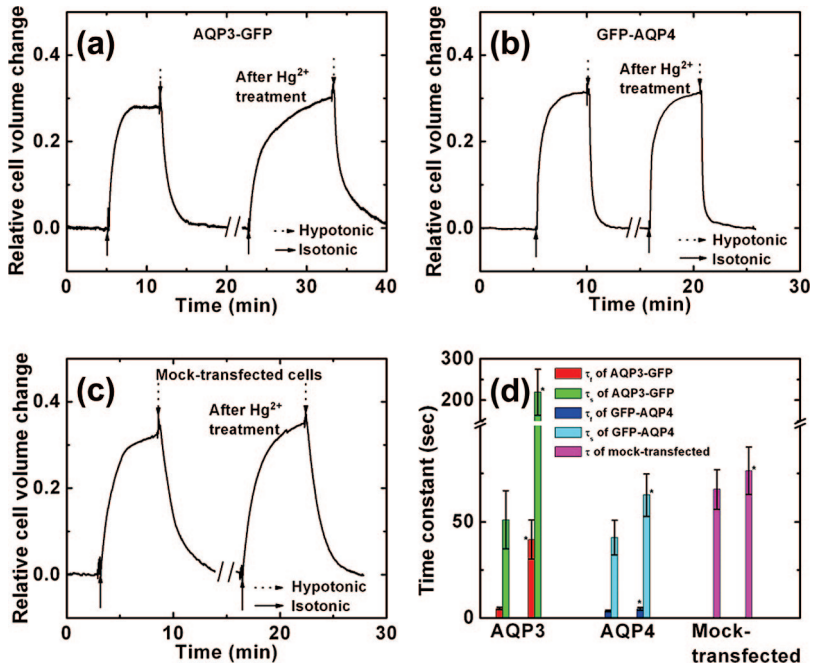

Figure 5. Effect of Hg^{2+} ion on the water transport in AQP3-expressing HEK cells (a), AQP4-expressing HEK cells (b), and mock-transfected HEK cells (c). (d) Graph showing the Hg^{2+} effect on the time constants obtained from the swelling curves shown in (a−c). After the first swelling curve of the cells was obtained, cells were treated with 0.1 μM Hg^{2+} in isotonic solution for 1 min and then rinsed with Hg^{2+}-free isotonic solution. The second swelling curve was obtained by perfusing Hg^{2+}-free hypotonic solution (256 mOsm). The bar graphs with one asterisk indicate the time constants obtained from the swelling curves after the Hg^{2+} treatment. The error bar represents 1σ of measurements from three independently prepared samples.

time constant was plotted in Figure 4d. The results showed that the τ_f values of AQP3- and AQP4-expressing cells as well as mock transfected cells were independent of the extracellular osmolarity. These data suggest that only osmotic water movement was involved in the fast phase swelling, and the water permeability through either AQPs or lipid bilayers should be independent of osmotic gradient across the membrane. The τ_s values of the AQP-expressing cells were not consistent for the different osmotic pressures. This suggests that other mechanisms, such as ion trafficking across the cell membrane and the influence of cytoskeleton, may contribute to the cell swelling during the repeated challenges. Various volume regulation mechanisms rely on different sensory signals and activation energy, and these effectors may be sensitive to membrane tension or cell volume. Several groups have reported the connection between AQP and ionic channel activity,[6,27] suggesting that the expression of AQP in the cells might also affect ionic transport pathways and RVD processes. Mock-transfected cells exhibited consistent τ values as shown in Figures 3 and 4, suggesting no significant water movement due to ions or other osmolytes transport.

Effect of Heavy Metal Ions on the Water Transport. To demonstrate the applicability of the cell volume sensor for AQP drug screening, we examined two heavy metal ions, Hg^{2+} and Ni^{2+}, for their selectivity and efficiency of blocking AQP3 and AQP4 channels.[24,28,29] Panels a−c in Figure 5 show the Hg^{2+} effect on the swelling of the AQP3- and AQP4- expressing cells and mock-transfected cells. After the first cycle of hypotonic and isotonic perfusion, the cells were perfused with isotonic solution containing 0.1 μM Hg^{2+} for 1 min and then rinsed with Hg^{2+}-free isotonic solution. The second swelling curve indicates the result of Hg^{2+} application. Figure 5d is a graph of time constants obtained from the swelling curves shown in Figure 5a−c. We and others previously found that a high concentration of Hg^{2+} (>50 μM) could rapidly alter the permeability of Na^+, K^+, and Cl^- ions, leading to extraordinary water flow across the cell membrane.[30,31] Therefore, we optimized the dose of Hg^{2+} to minimize the side effect of Hg^{2+}. As shown in Figure 5a and d, after the Hg^{2+} treatment, the water transport rate in the AQP3-expressing cells have been greatly reduced. Both the τ_f and τ_s values were increased up to 8× and 4×, respectively. While the effect of Hg^{2+} on the fast phase swelling can be easily explained by the mercurial inhibition of AQP, its effect on the slow phase swelling is more complicated, involving the interaction between Hg^{2+} and other membrane protein channels. The application of Hg^{2+} (even with low dose) could promote Na^+ uptake and KCl efflux that could modify the water permeability in the slow phase. In comparison, the τ_f and τ_s values of AQP4-expressing cells were not affected by the Hg^{2+}. It is known that Hg^{2+} irreversibly binds to the cysteine group in the pore of the AQP3 and blocks the pore.[28] The irreversible binding property of Hg^{2+} in the AQP3 sites was characterized by observing that the repeated Hg^{2+}-free hypotonic perfusion did not restore the swelling rate of the first swelling curve (data not shown). On the contrary, since AQP4 lacks a cysteine in the corresponding site, Hg^{2+} does not show an inhibitory effect for the AQP4.[29] As a control, we examined the Hg^{2+} effect on water

(27) Liu, X.; Bandyopadhyay, B.; Nakamoto, T.; Singh, B.; Liedtke, W.; Melvin, J. E.; Ambudkar, I. *J. Biol. Chem.* **2006**, *281*, 15485–15495.
(28) Kuwahara, M.; Gu, Y.; Ishibashi, K.; Marumo, F.; Sasaki, S. *Biochemistry* **1997**, *36*, 13973–13978.
(29) Hasegawa, H.; Ma, T.; Skach, W.; Matthay, M. A.; Verkman, A. S. *J. Biol. Chem.* **1994**, *269*, 5497–5500.
(30) Rothstein, A.; Mack, E. *Am. J. Physiol. Cell Physiol.* **1991**, *260*, C113–C121.
(31) Heo, J.; Meng, F. J.; Sachs, F.; Hua, S. Z. *Cell Biochem. Biophy.* **2008**, *51*, 21–32.

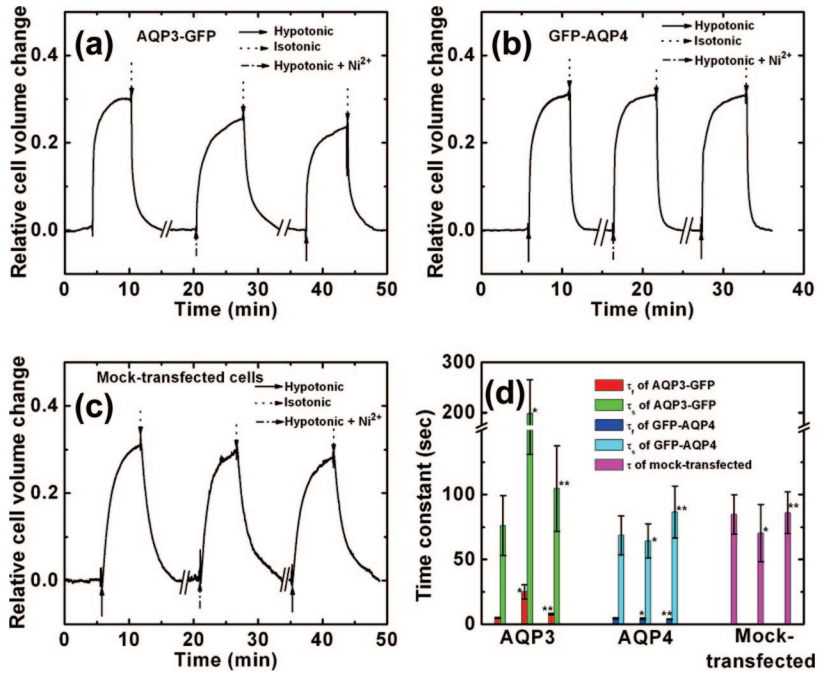

Figure 6. Effect of Ni^{2+} ion on the water transport in AQP3-expressing HEK cells (a), AQP4-expressing HEK cells (b), and mock-transfected HEK cells (c). (d) Graph showing the Ni^{2+} effect on the time constants obtained from the swelling curves shown in (a−c). In (a)−(c), The first and the third swelling curves were obtained using normal hypotonic (256 mOsm) solution. The second swelling curve was obtained using hypotonic (256 mOsm) containing 1 mM Ni^{2+}. The baseline for the second swelling curve was obtained using isotonic solution containing 1 mM Ni^{2+}. The bar graphs with one and two asterisks indicate the time constants obtained from the second and third swelling curves, respectively. The error bar represents 1σ of measurements from three independently prepared samples.

transport in the mock-transfected cells. As shown in Figure 5c and d, the Hg^{2+} treatment did not change the τ values significantly, suggesting relative low expression of AQP3 in the control cells.

Similarly, the Ni^{2+} effect on cell swelling was displayed in Figure 6a−c. After obtaining the first swelling curve in normal hypotonic solution, the second swelling curve was obtained in the hypotonic solution containing 1 mM Ni^{2+}. To eliminate the effect of change in the solution conductivity on the signal, the baseline for the second swelling curve was obtained using the isotonic solution containing 1 mM Ni^{2+}. The third curve was obtained using Ni^{2+}-free normal hypotonic solution after rinsing the cells with Ni^{2+}-free isotonic solution. Figure 6d is a graph of time constants obtained from the swelling curves in Figure 6a−c. Panels a and d in Figure 6 show that both τ_f and τ_s values of AQP3-expressing cells was noticeably increased in the Ni^{2+}-containing hypotonic solution. After rinsing the cells, the time constants of the AQP3-expressing cells were restored close to the initial τ values, indicating that Ni^{2+} reversibly blocks the AQP3 channel. In comparison, Ni^{2+} did not significantly affect the water permeability of AQP4-expressing cells. These observations are consistent with the previous finding:[24] Ni^{2+} can bind to three amino acid residues leading to the AQP3 blocking; however, because the three amino acids are replaced with other amino acids in the corresponding sites of AQP4, Ni^{2+} does not show an inhibitory effect for the AQP4. Mock-transfected cells did not show a noticeable change in the time constant in the presence of Ni^{2+}, confirming low expression level of AQP3 in the control cells.

CONCLUSIONS

In this report, we examined the participation of AQPs in the water transport using an impedance-based microfluidic cell volume sensor. We compared the time-resolved water transport characteristics between AQP-gene transfected cells and mock-transfected cells and demonstrated the significance of AQPs' role in the osmotic water transport. We also showed the applicability of the sensor for screening AQP-specific drugs by demonstrating that the water permeability of AQPs can be selectively modulated using heavy metal ions, such as Hg^{2+} and Ni^{2+}. Microfluidic sensor chip provides the benefit of fast solution exchange and small consumption of reagents. We anticipate that a high-throughput assay will be possible by incorporating parallel array design into the volume sensor.

SUPPORTING INFORMATION AVAILABLE

Figure SI: (a) Confocal fluorescence micrograph showing distribution of AQP3 expressed in HEK-293 cells. AQP3 tagged with GFP is localized in the plasma membranes of the transfected cells. (b) Confocal fluorescence micrograph showing distribution of AQP4 expressed in HEK-293 cells. AQP4 tagged with GFP is localized in the plasma membranes of the transfected cells. The micrographs were obtained with an LSM510 META confocal microscope (Carl Zeiss, Jena, Germany) using 488-nm Ar ion laser and GFP filter set. An oil-merged 63×, 1.4 numerical aperture apochromat objective lens (Carl Zeiss) was used. This material is available free of charge via the Internet at http://pubs.acs.org.

ACKNOWLEDGMENT

This work was supported by National Institute of Health Grant DK77302 and by New York State Office of Science, Technology & Academic Research (NYSTAR). We thank Prof. Frederick Sachs for providing the AQP-encoding genes and helpful comments on this project.

Received for review April 26, 2008. Accepted July 4, 2008.

AC8008498